

ION BEAMS FROM HIGH-CURRENT PF FACILITIES

M. Sadowski

Soltan Institute for Nuclear Studies, 05-400 Otwock-Świerk n. Warsaw, Poland

Abstract: The paper concerns pulsed beams of fast deuterons and impurity- or admixture-ions emitted from high-current PF-type facilities operated in different laboratories. A short comparative analysis of time-integrated and time-resolved studies is presented. Particular attention is paid to the microstructure of such ion beams, and to the verification of some theoretical models.

1. Introduction

Ion beams generated in PF facilities have been investigated in many laboratories, using different diagnostic techniques, e.g., nuclear-activation methods [1-3], magnetic ion spectrometers [4], Thomson-type analyzers [5-6], and time-of-flight measuring systems [7-8]. General characteristics of high-energy (>100 keV) deuterons beams, e.g., their angular distribution and energy spectra, have been studied by several authors [5-10]. Energy distributions of impurity (as nitrogen, oxygen) and admixture (as argon) ions in various ionization states have also been investigated [6]. Some attention has been devoted to temporal characteristics of ion pulses [8, 10] and their correlations with other PF phenomena [10-13].

The main aim of this paper has been to compare the ion emission characteristics of several PF facilities, to bring attention to the microstructure of such ion beams, and to comment on different physical models of the ion acceleration.

2. Analysis of experimental results

As regards a total amount of fast primary deuterons, accelerated and emitted from PF discharges performed with a deuterium filling, it has been shown that at a stored energy of about 70 kJ more than 10^{15} deuterons are accelerated to energy above 300 keV, and more than 10^{12} deuterons reach energy of several MeV [3, 6]. It has also been measured that within a 56-kJ PF-device the deuteron energy distribution decreases exponentially from about 300 keV to about 3 MeV [6], and within a larger 280-kJ PF-facility this exponential decrease is steeper and extends to 2 MeV only [14], while the total number of deuterons above 70 keV is about the same (up to 10^{12} sr⁻¹ end-on and up to 10^{11} sr⁻¹ side-on). In general, deuteron energy distributions depend strongly on the initial operational pressure. At lower initial pressures an increase in the X-ray and primary-ion emission is usually observed, and sometimes two different types of ion energy spectra are detected, as shown in Fig.1. It should also be noted that an exponential decay of the deuteron energy distribution was observed in many PF-devices, e.g. [4, 6, 12], while very energetic deuterons (up to about 10 MeV) were registered in a few experiments only [12].

As regards impurity- and admixture-ions, they have been analyzed with Thomson-

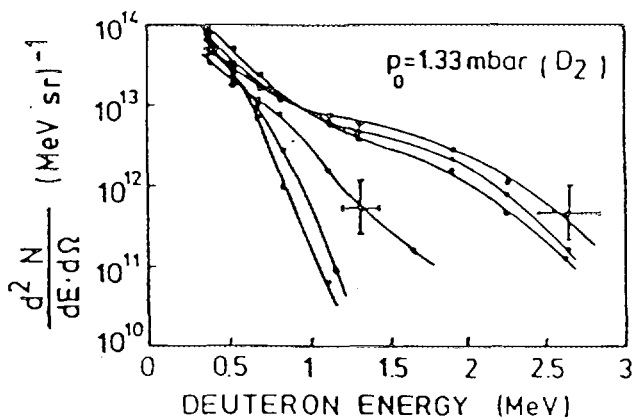


Fig.1. Deuteron energy distributions obtained from several discharges within a 56-kJ PF device [6] operated at low initial pressure.

type mass-spectrometers [6, 12, 16], as shown in Fig.2. Their energy distributions can be described by an exponential rise and an exponential decay with the maximum ranging from $E/Z = 0.8$ MeV to 1.3 MeV. The spectra of the highly ionized species (with $Z > 4$) extend to the value of $E/Z = 1.8-1.9$ MeV, while the lower ionized impurities (with $Z < 4$) reach somewhat higher value $E/Z = 2-2.8$ MeV. It can be concluded that the similarity of energy distributions for different ion species, and proportionality of their maximum energy to electrical charge, indicate that impurity (admixture) ions are accelerated by similar processes involving strong electric fields.

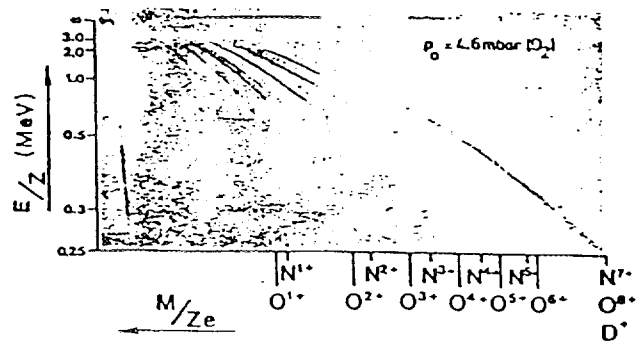


Fig.2. Typical ion spectra, as registered with a Thomson-type analyzer and nuclear track detector for a single shot within a 56-kJ PF device [16] operated at higher initial pressure.

Taking into account that ion emitting regions (sources) are of the submillimeter range, as deduced from the ion pinhole pictures [5], local electric field intensity can reach above 50 MV/cm. This value is much higher than that induced by rapid changes in inductance of the electrical circuit. Let us consider $E_{ind} = I dL/dt$, where $L = \mu/2\pi \ln R/r(t)$, R - the maximum radius, $r(t)$ - the radius of a current sheath. Hence $E_{ind} = B_\phi dr/dt$, where the magnetic field $B_\phi = I \mu/2\pi r$. Substituting $I = 10^5$ A, $R = 2.5$ cm, $r_{min} = 5 \times 10^{-3}$ cm, $(dr/dt)_{max} = 3.5 \times 10^7$ cm/s, one gets $E_{ind} = 1.4$ MV/cm only. Therefore, the direct acceleration of charged particles to energy within a MeV region by the pinch-induced electrical fields is impossible, and other mechanisms have to be considered.

In order to shed some light on dynamics of the ion emission time-resolved measurements have been performed with different PF facilities [8, 11, 12]. Using an ion pinhole camera and miniature scintillation detectors placed in different points of a space-resolved ion image [10], it has been shown that the ion pulses reveal a coarse (~ 30 ns) and a fine (~ 2 ns) structure. Also mass- and energy-resolved measurements, as performed by means of a Thomson-type analyzer equipped with scintillation detectors, have demonstrated the multi-spike structure of ion pulses, e.g., for quasi-monoenergetic deuterons there were registered 3 separate pulses coming within 30-40 ns time intervals. It can be explained on the basis of a model assuming that fast deuterons (ions) are emitted from different microsources [9], in a form of numerous beams of various energy, at different instants after the current peculiarity.

The hypothesis about ion microbeams has been confirmed by detailed studies performed with ion pinhole cameras equipped with nuclear track detectors covered with different absorption filters. Typical ion pinhole pictures, demonstrating quasi-concentric structures composed of

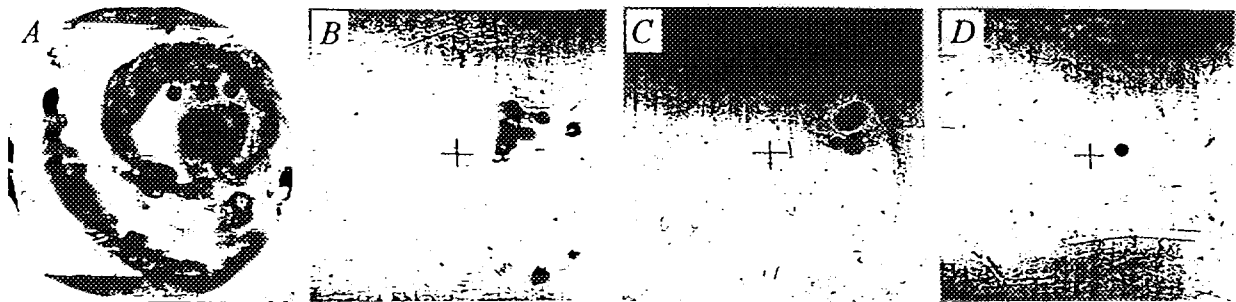


Fig.3. Ion pinhole pictures, as taken end-on by means of CN-films covered with different Al-filters: A - 1.5- μ m Al-filter, $E_d > 220$ keV; B - 6.0- μ m Al-filter, $E_d > 700$ keV; C - 20.0- μ m Al-filter, $E_d > 1.7$ MeV; and D - 30- μ m Al-filter, $E_d > 2.1$ MeV.

numerous microbeam spots [5], have been obtained only with thin ($<3 \mu\text{m}$) Al-filters. With thicker filters the ion pinhole pictures demonstrated the deuteron microbeams, as shown in Fig. 3. It is worthy to mention that an angular divergence of such ion microbeams, as measured by direct methods (2 ion pinhole cameras situated one behind the other), was found to be rather small ($<8^\circ$).

In order to explain the ion emission different acceleration mechanisms have been considered by many authors, e.g. in [16-17] and numerous Refs. *ibid.* Some researchers apply a simple plasma-diode model, while other prefer more complicated models which involve various instabilities, e.g., electron cyclotron drift instability etc. Considering angular distributions of ions emitted from PF discharges, it should be noted that in several experiments of different energetics (ranging from 3.6 kJ to above 200 kJ) there were observed: asymmetry in relation to the z-axis, a considerable decrease in the ion emission at Θ -angles higher than $20\text{-}40^\circ$, and characteristic emission dip at given angle (at $\Theta=0^\circ$ in PGN device, and at $\Theta=20^\circ$ in PF-360 facility) [18]. These features have also been observed in the PF-1000 device [19], as shown in Fig. 4.

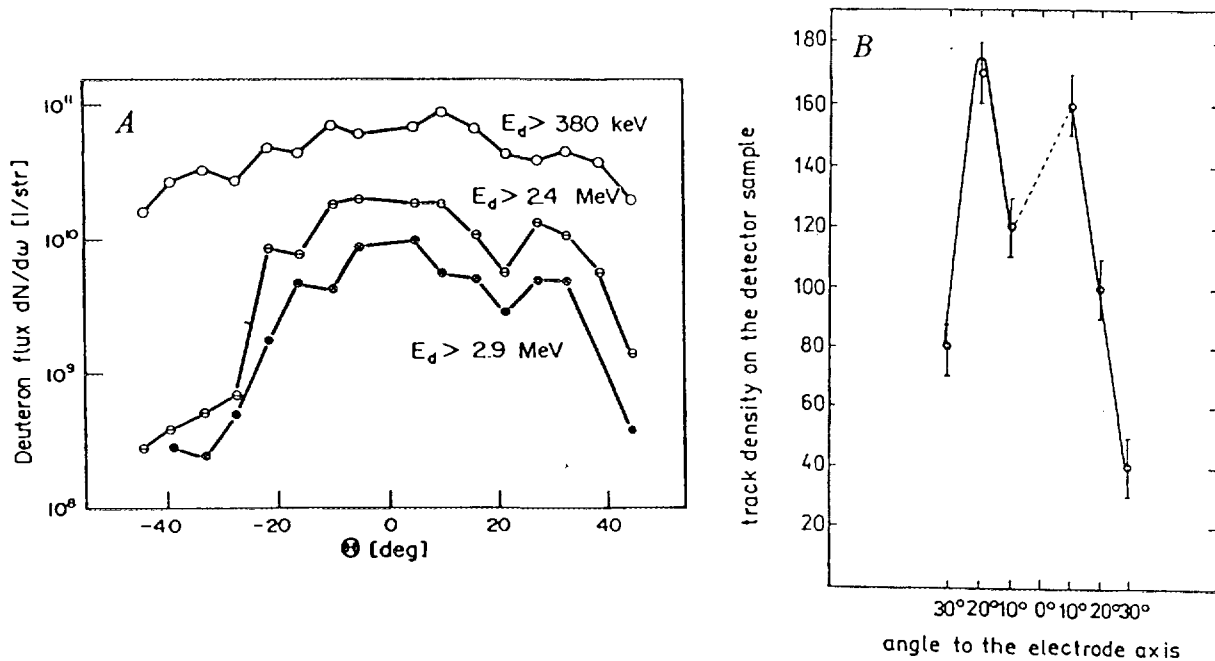


Fig.4. Angular distributions of high-energy deuterons, as obtained (A) for 126-kJ shots within the PF-360 device, and (B) for 240-kJ discharges within the PF-1000 facility.

With a pinch column surrounded by an azimuthal magnetic field, 2D calculations of ion trajectories (even without taking into account filamentation effects) show that an angular anisotropy is an inherent feature of all the PF discharges. Also deviations from axial symmetry can easily be explained by the stochastic formation of the ion microsources and by heterogeneity of local electromagnetic fields. The ion-emission minima (dips) observed at given angles might be connected with the lack of accelerated particles within a hole of an ion larmor diameter. Considering the minimum pinch radius and pinch current intensity one can estimate the magnetic field at the pinch surface, e.g., for $r_{\text{min}} = 2 \text{ mm}$, $I_p = 800 \text{ kA}$, $B_{\text{max}} = 800 \text{ kG}$. Under such conditions even 500-keV deuterons (with $r_L = 1.3 \text{ mm}$) can be confined (trapped) by the current sheath, and along the pinch axis one can observe an ion emission dip. The pinch axis does not necessarily correspond to the z-axis of the PF facility.

Considering ion beams emitted from a focus region, one must take into account the attenuation of those in the focus region, and after that the slowing-down of deuterons by a neutral gas layer in front of a detector plate. These effects can be computed for different deuteron energies, as shown in Fig 5.

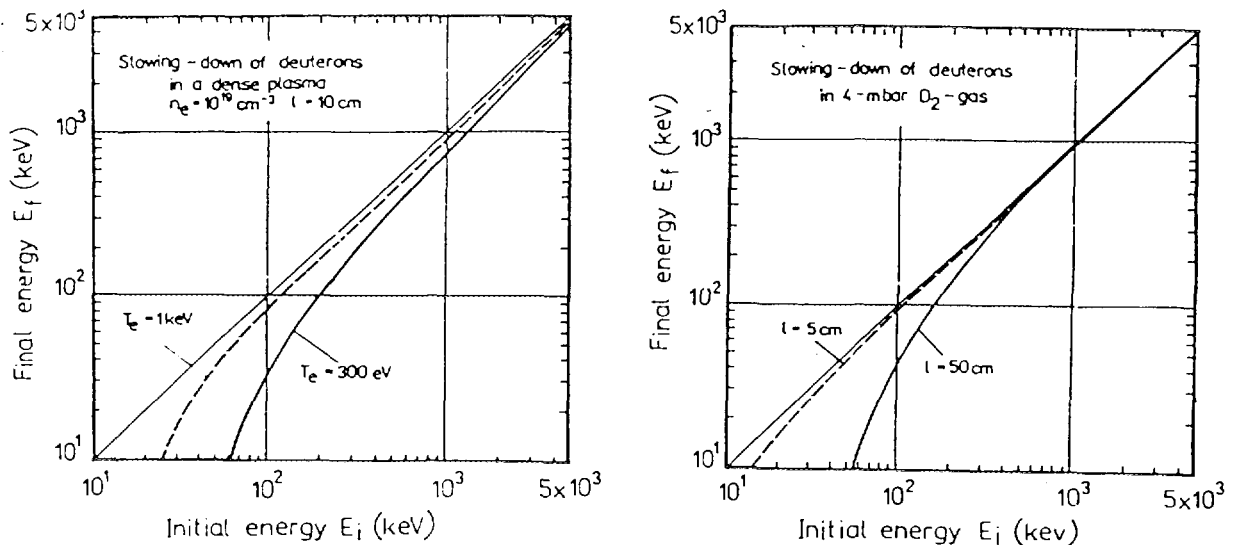


Fig. 5. Diagrams presenting the attenuation of deuterons by a dense plasma within a focus region (on the left), and by neutral D_2 gas between the focus and a detector plane (on the right).

3. Summary and conclusions

The most important conclusions from this analysis can be formulated as follows:

1. Anisotropy in the ion emission from PF discharges can be explained by the fact that ion microsources (depending on local plasma parameters and fields) are formed stochastically and with a large symmetry jitter in relation to the z -axis.
2. The first mechanism of the ion acceleration can be attributed to ion reflections inside the collapsing current sheath (funnel) and to electrical fields generated inductively. Mechanisms of the generation of subsequent fast ion pulses are more complicated, and they are connected possibly with microturbulences and electric fields induced by decaying plasma microstructures.
3. Particular attention should be paid to studies of time correlations. Experimental data collected so far are insufficient to identify all the physical processes involved in the formation of the pinch column and the ion microsources.

References

- [1] Ch.Maisonnier, J.P.Rager; Proc. 3rd Int. Conf. High-Power Electron and Ion Beams (Novosibirsk 1979), Inv. Paper.
- [2] N.V.Filippov, T.I.Filippova; JETP Lett. **25** (1977) 241.
- [3] R.L.Gullickson, H.L.Sahlin; J. Appl. Phys. **49** (1978) 1099.
- [4] H.Krompholz, L.Michel, K.H.Schonbach, N.Fisher; Appl. Phys. **13** (1977) 29.
- [5] L.Bertalot, H.Herold, U.Jager, et al.; Phys. Lett. **79A** (1980) 389.
- [6] A.Mozer, M.Sadowski, H.Herold, H.Schmidt; J. Appl. Phys. **53** (1982) 2959.
- [7] R.L.Gullickson, J.W.McClure, W.L.Pickles, et al.; Proc. Int. Conf. Plasma Sci. (Madison 1980), p.75.
- [8] G.Gerdin, W.Stygar, F.Venneri; J. Appl. Phys. **52** (1981) 3269.
- [9] L.Bertalot, R.Deutsch, H.Herold, et al.; Proc. 10th Europ. Conf CFPP (Moscow 1981), p.D-1.
- [10] M.Sadowski, J.Zebrowski, E.Rydygier, et al.; Phys. Lett. **113A** (1985) 25.
- [11] K.Hirano, T.Yamamoto, K.Shimoda, H.Nakajima; J. Phys. Soc. Jap. **58** (1989) 3591.
- [12] W.H.Bostick, H.Kilic, V.Nardi, C.W.Powell; Nucl. Fusion **33** (1993) 413.
- [13] M.Sadowski, J.Baranowski, L.Jakubowski, et al.; Proc. 21st EPS Conf CFPP (Montpellier 1994), p.1320.
- [14] H.Herold, L.Bertalot, U.Jager, et al.; Proc. 14th EPS Conf. CFPP (Aachen 1983), p.477.
- [15] H.Herold, A.Mozer, M.Sadowski, H.Schmidt; Rev. Sci. Instrum. **52** (1981) 24.
- [16] S.P.Gary, F.Hohl; Report LA UR78-518 (1978).
- [17] K.G.Gureev; Sov. Phys. Tech. Phys. **25** (1980) 192.
- [18] M.Sadowski, J.Zebrowski, E.Rydygier, J.Kucinski; Plasma Phys. Contr. fusion **30** (1988) 763.
- [19] M.Scholz and PF-1000 Team; Proc. 2nd Nat. Symp. PLASMA'95 (Warsaw 1995), Vol.11, p.15.